ELSEVIER

Journal of Chromatography A, 838 (1999) 179–189

JOURNAL OF CHROMATOGRAPHY A

DNA–histidine complex formation in isoelectric histidine buffers

Nancy C. Stellwagen[a,*], Cecilia Gelfi[b], Pier Giorgio Righetti[c]

[a]*Department of Biochemistry, University of Iowa, Iowa City, IA 52242, USA*
[b]*ITBA, CNR, Via Fratelli Cervi No. 93, Segrate 20090, Milan, Italy*
[c]*Department of Agricultural and Industrial Biotechnologies, University of Verona, Strada Le Grazie, Ca' Vignal, 37134 Verona, Italy*

Abstract

The free solution electrophoretic mobility of two DNA molecules of different molecular masses, 18 base pairs and 2686 base pairs, has been measured in isoelectric histidine buffers with and without added low-molecular-mass electrolytes. Extensive DNA–histidine complex formation is observed in isoelectric histidine buffer, as evidenced by distortion and splitting of the peaks in the electropherograms. Peak distortion and splitting can be decreased or eliminated by adding low-molecular-mass neutral salts to the solution, suggesting that the DNA–histidine complexes are stabilized by electrostatic interactions. The ability of various neutral salts to disrupt the DNA–histidine complexes depends on the molecular mass of the DNA and the concentration and type of added salt.

Keywords: Complexation; Buffer composition; DNA; Histidine

1. Introduction

Isoelectric buffers are beginning to find applications in capillary zone electrophoresis, because the very low conductivity of the buffers at their isoelectric pH allows very high electric fields to be applied to the capillary, decreasing the separation time [1–5]. Single-stranded DNA oligomers have been studied in three different isoelectric buffers: histidine [2], lysine [3] and IDA (iminodiacetic acid) [4]. The capillaries were filled with sieving liquid polymers in order to separate the DNA, because high-molecular-mass DNA molecules migrate with identical mobilities in free solution [6,7]. At neutral pH, the most efficient separations of single-stranded DNA molecules were obtained in isoelectric histidine buffer containing 7 *M* urea [2–5].

The separation of double-stranded (ds) DNA molecules has recently been carried out in isoelectric histidine buffer in capillaries filled with liquid polyacrylamide {4–6% T, 0% C; T=[g acrylamide+g *N,N′*-methylenebisacrylamide (Bis)]/100 ml solution; C=g Bis/% T} [8]. Good resolution was observed for DNA fragments smaller than 125 base pairs (bp); baseline separation of fragments up to 587 bp in size was accomplished by adding low-molecular-mass electrolytes to the isoelectric histidine buffer [8]. It was postulated that isoelectric histidine forms complexes with DNA, which can be disrupted by adding neutral salts to the buffer.

In this work, DNA–histidine complex formation in isoelectric histidine buffers has been studied in more detail. The capillary was filled with buffer alone; no sieving liquid polymers were added. Two dsDNA samples were used, a high-molecular-mass sample of linearized pUC19 (2686 bp) and a low-molecular-mass, 18 bp oligomer, in order to investi-

*Corresponding author. Tel.: +1-319-335-7896; fax: +1-319-335-9570.

0021-9673/99/$ – see front matter
PII: S0021-9673(99)00049-7

gate the molecular mass dependence of the mobility in this buffer medium. Molecular mass-dependent mobilities have been previously been observed for small single-stranded [9] and double-stranded [7,10] DNA molecules in Tris–acetate (TAE) and Tris–borate (TBE) buffers in free solution.

The results described here confirm that extensive complex formation occurs between histidine and dsDNA molecules in isoelectric histidine buffers. Complex formation can be reduced or eliminated by adding monovalent cations to the solution. The stability of the DNA–histidine complexes depends on the concentration and type of added neutral salt, as well as the molecular mass of the DNA.

2. Experimental

2.1. DNA samples

Linearized pUC19 was prepared by digestion of the supercoiled plasmid with the restriction enzyme *Bsa*I, according to the manufacturers' instructions. After digestion was complete, as monitored by agarose gel electrophoresis [11,12], the linearized DNA was ethanol precipitated, dissolved in T0.1E buffer (10 m*M* Tris–HCl, pH 8.1, plus 0.1 m*M* EDTA) at a concentration of ~200 ng/μl, and stored at −20°C. The ds18-mer, which was >98% pure, had the sequence 5′-ACGATCACCTTTGCTCAC-3′. The individual oligonucleotides were synthesized by standard methods, purified by reverse-phase HPLC, annealed and stored at 4°C as a 100 μ*M* stock solution in distilled water. The two DNA stock solutions and various mixtures were diluted to the required concentration with T0.1E buffer (defined above). Unless otherwise indicated, the pUC19 concentration in the injected solutions was always 75 ng/μl; the concentration of the 18-mer was 30 ng/μl. The DNAs in the mixtures were identified by the relative areas of the peaks in the electropherogram and/or by running the components separately.

2.2. Electrophoresis buffers

The running buffer used for most of the experiments was 50 m*M* histidine, used at its isoelectric pH of 7.7. No acid or base was added to adjust the pH. Various monovalent and divalent salts were added to this buffer, as described below. Control experiments were carried out using 40 m*M* TAE buffer (40 m*M* Tris acetate, 1 m*M* EDTA, pH 8.0 [12]). All buffers were prepared with doubly distilled water, filtered by suction through a 0.22-μm Millipore filter (Bedford, MA, USA), and stored at 4°C until needed.

2.3. Apparatus

Capillary zone electrophoresis was carried out using a Beckman P/ACE System 5000 apparatus (Fullerton, CA, USA), operated in the reverse polarity mode with UV detection at 254 nm, close to the absorption maximum of DNA. Elution times and peak profiles were calculated with the GOLD software program. Polyacrylamide coated capillaries (Beckman, eCAP) with external diameters of 375 μm, internal diameters of 100 μm and lengths of 27.0 cm (20.2 cm to the detector) were used. The electroendosmotic flow (EOF) in the capillaries was determined by direct measurements with 20 m*M* acrylamide, using normal instrument polarity and detection at 214 nm. The EOF mobility was always $\leq 1 \cdot 10^{-5}$ cm^2 V^{-1} s^{-1} and could be neglected when calculating the mobilities of the DNA molecules.

The DNA samples were injected into the capillary by a 1 s injection at low pressure (0.5 p.s.i., 0.007 MPa), using methods described previously [7]. The injection volume was 18.6 nl; the plug length was 2.4 mm. Between runs, the capillary was rinsed with running buffer for 1 min at high pressure (0.28 MPa, >20 column volumes). The capillaries were flushed with distilled water using an HPLC pump (Beckman model 110A) at the end of each day and filled with distilled water overnight.

DNA electrophoretic mobilities, μ, were calculated from Eq. 1:

$$\mu = d/Et \quad (1)$$

where d is the distance to the detector (in cm), E is the electric field strength (in V/cm) and t is the time required for the sample to migrate to the detector (in s). All measurements were carried out at 25.0±0.1°C, using $E = 50$ or 100 V/cm. Heating of the liquid-cooled capillary was negligible at these low electric field strengths; the temperature differ-

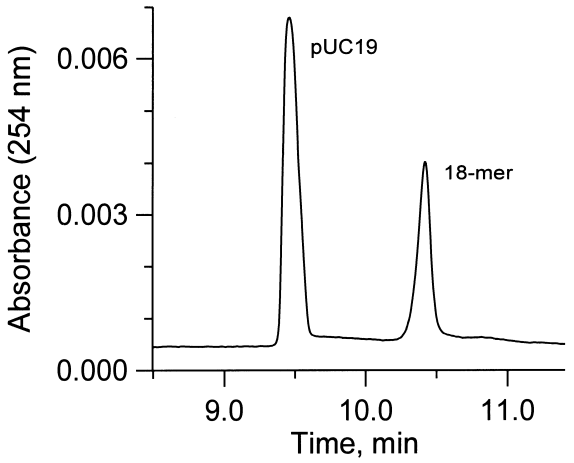

Fig. 1. Elution profiles of linear pUC19 and the 18-mer in 40 m*M* TAE buffer. The absorbance at 254 nm is plotted as a function of elution time; $E=100$ V/cm, $I=10.8$ μA.

ence between the center and the outer edge of the capillary was estimated to be ≤0.4°C, even in the most highly conducting solutions used here. The measured current in the capillary was always proportional to the applied voltage, another indication that Joule heating was negligible. The apparent absolute electrophoretic mobilities were generally reproducible within $\pm 0.03 \cdot 10^{-4}$ cm^2 V^{-1} s^{-1} in TAE buffer and $\pm 0.1 \cdot 10^{-4}$ cm^2 V^{-1} s^{-1} in isoelectric histidine buffer, regardless of DNA concentration, electric field strength and/or the age of the capillary. Identical results were also obtained with two different eCAP capillaries. Control measurements were carried out by injecting sample buffer (T0.1E) without DNA into the capillary.

3. Results

3.1. Electrophoresis of linear pUC19 and the ds18-mer in TAE buffer

The electropherogram of a mixture of linear pUC19 and the ds18-mer in 40 m*M* TAE buffer is illustrated in Fig. 1. Two peaks with nearly Gaussian shapes were observed, well separated in elution time. The two peaks can be identified by their relative areas, since the two DNAs were injected with different nucleotide concentrations. The identification was confirmed by running linear pUC19 separately. The electrophoretic mobility of the faster peak, corresponding to linear pUC19, was $(3.59\pm0.03)\cdot 10^{-4}$ cm^2 V^{-1} s^{-1}. The slower peak, corresponding to the 18-mer, had a mobility of $(3.29\pm0.03)\cdot 10^{-4}$ cm^2 V^{-1} s^{-1}. These mobilities are in excellent agreement with previous results [7]. The mobilities were also independent of concentration over the range tested (two-fold for linear pUC19; 20-fold for the 18-mer) and electric field strength, *E*, over a four-fold variation in *E*.

3.2. Electrophoresis of the two DNAs in 50 mM isoelectric histidine buffer

Completely different results were observed in 50 m*M* histidine buffer, as shown in Fig. 2. The two DNAs and their mixture exhibited two peaks, a broad, relatively rapidly migrating peak eluting at 16–17 min, and a slower, sharper peak eluting at 26–33 min, depending on the particular DNA in the sample. Both peaks contained DNA, since histidine

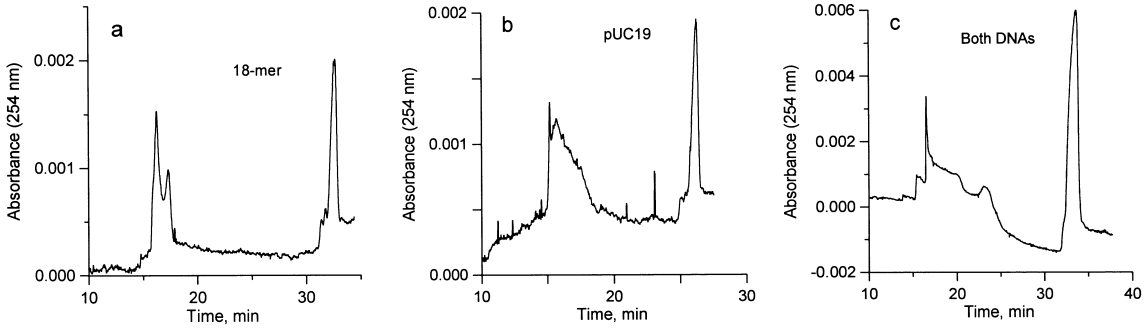

Fig. 2. Electropherograms observed in isoelectric 50 m*M* histidine buffer, pH 7.7, for (a), the 18-mer; (b), linear pUC19; (c), a mixture of the two DNAs. In all cases, $E=50$ V/cm, $I=0.8$ μA. Equal amounts of DNA were injected in each sample.

does not exhibit an appreciable absorbance at 254 nm [13]. Since injection of the sample buffer (T0.1E) without DNA into the capillary resulted in a flat electropherogram with no peaks, the sample buffer did not contribute to the spectral features observed in Fig. 2. The broadening of the peaks and splitting into two components (Fig. 2) are unmistakable evidence of DNA–histidine complex formation, since single peaks with nearly Gaussian peak shapes were always observed in TAE buffer (Fig. 1) and TBE buffer [7]. The mobilities calculated for the rapidly- and slowly-migrating peaks in isoelectric histidine buffer are given in Table 1.

3.3. Electrophoresis in 50 mM histidine–NaCl solutions

To investigate the effect of neutral salts on the formation of DNA–histidine complexes, various concentrations of NaCl were added to 50 m*M* histidine buffer. Typical electropherograms observed for linear pUC19 are illustrated in Fig. 3. Single peaks were observed for this DNA in solutions containing 20–50 m*M* NaCl–50 m*M* histidine, becoming increasingly more symmetrical with increasing NaCl concentration. The elution times also gradually increased with increasing NaCl concentration, indicating that the electrophoretic mobility decreased with increasing solution conductivity, as expected from theoretical considerations [14,15]. The observed mobilities are summarized in Table 1.

Typical electropherograms observed for the 18-mer in running buffers containing 20–50 m*M* NaCl plus 50 m*M* histidine are illustrated in Fig. 4. The electropherogram observed in 20 m*M* NaCl–50 m*M* histidine appeared to be normal (Fig. 4a), although some instability in the baseline was observed at ~30 min. Two peaks were observed when the NaCl concentration was raised to 30 m*M* NaCl, as shown in Fig. 4b. A single peak was observed again in 50

Table 1
Electrophoretic mobilities observed in 50 m*M* isoelectric histidine buffer with added neutral salts

Added salt	Concentration (m*M*)	18-mer[a]		pUC19[a]		Mixture[a]	
		Fast peak	Slow peak	Fast peak	Slow peak	Fast peak(s)	Slow peak(s)
None	0	4.1	2.2	4.2	2.4	4.2	2.1
NaCl	10	4.3	–	5.3	–	4.7, 5.0	–
	20	3.3	–	4.2	–	3.3, 4.1	2.2
	30	3.3	2.4	4.0	–	3.2, 4.1	2.4
	50	2.6	–	3.4	–	2.6, 3.3	–
KBr	10	4.1	2.5	4.8	2.1	4.5	2.4
	30	2.9	1.9	4.1	2.1	3.1, 3.8	2.0
	50	3.4	2.6	4.4	2.5	3.3, 4.2	2.5
	60	2.9	–	3.8	2.0	2.8, 3.8	2.1
	50[b]	2.7	–	3.8	1.9	2.8, 3.7	1.9
Na_2SO_4	30	3.0	2.2	3.9	2.2	3.1, 3.9	2.3
$CaCl_2$	10	2.5	1.8	2.5	1.7	2.6	1.9
	20	2.3	1.6	–	1.8	2.4	1.6
$CaCl_2$	30	1.8	1.2	1.8	1.3	1.8	1.1, 1.2
TAE buffer[c]	40	–	–	3.60	–	3.25, 3.59	–

[a] Mobility $\cdot 10^4$ cm^2 V^{-1} s^{-1}; the standard deviation is $\pm 0.1 \cdot 10^4$ cm^2 V^{-1} s^{-1}.
[b] 25 m*M* isoelectric histidine buffer.
[c] Without isoelectric histidine buffer.

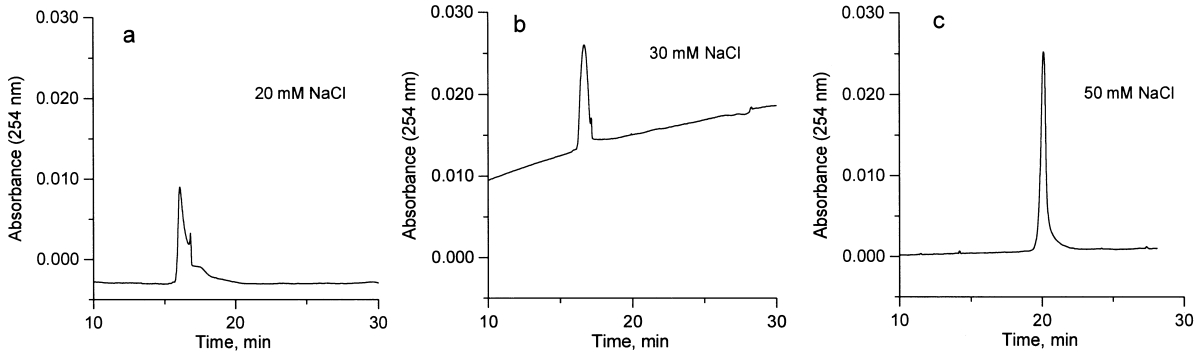

Fig. 3. Electropherograms of linear pUC19 in 50 m*M* histidine containing: (a), 20 m*M* NaCl, $I=10.2$ μA; (b), 30 m*M* NaCl, $I=13.1$ μA; (c), 50 m*M* NaCl, $I=24.0$ μA. In all cases, $E=50$ V/cm. Note that the scale is the same for all spectra, to facilitate visual comparisons. The rising baseline in (b) was due to incomplete lamp warmup.

m*M* NaCl–50 m*M* histidine, as shown in Fig. 4c. The absolute mobilities of the various peaks are compiled in Table 1.

Mixtures of the two DNAs exhibited somewhat more complicated electropherograms, as shown in Fig. 5. In solutions containing 50 m*M* NaCl–50 m*M* histidine (Fig. 5c), the elution profile contained two peaks, as expected from the elution profiles of the two individual components (compare Figs. 3c and 4c). However, differences were observed at lower NaCl concentrations, especially in 20 m*M* NaCl/50 m*M* histidine (Fig. 5a), where three peaks were observed in the electropherogram. The two faster migrating peaks had the elution times expected for the individual DNA components (compare Figs. 3a and 4a). However, a slowly migrating peak with an elution time of ~30 min was also observed; this peak had no counterpart in the spectra of the individual DNAs. Three peaks were also observed for the mixture of DNAs in 30 m*M* NaCl–50 m*M* histidine (Fig. 5b). Again, the two faster-migrating peaks correspond to the elution times observed for the individual DNAs (compare Figs. 3b and 4b); the slow peak corresponds to the slow peak observed in the electropherogram of the 18-mer (Fig. 4b).

3.4. Electrophoresis in isoelectric histidine–KBr solutions

Similar experiments were carried out with various concentrations of KBr added to 50 m*M* histidine. KBr was chosen because the limiting equivalent

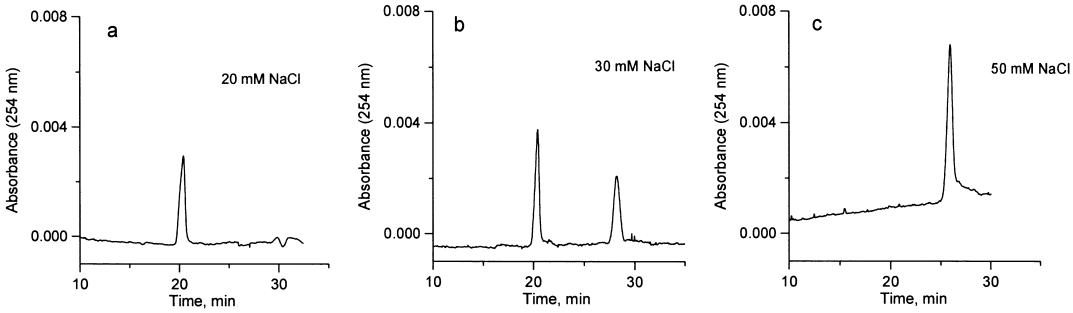

Fig. 4. Electropherograms of the 18-mer in 50 m*M* histidine containing: (a), 20 m*M* NaCl, $I=10.1$ μA; (b), 30 m*M* NaCl, $I=14.1$ μA; (c), 50 m*M* NaCl, $I=24.0$ μA. In all cases, $E=50$ V/cm. The occasional vertical spikes were due to bubble formation.

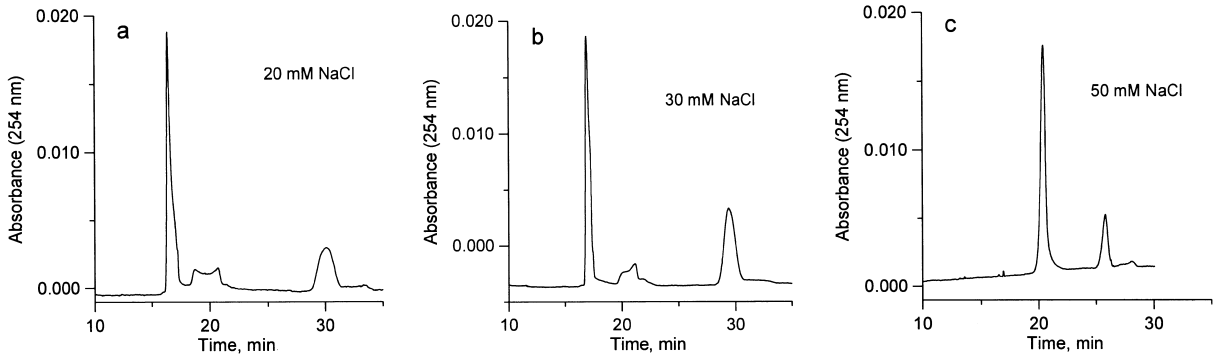

Fig. 5. Electropherograms of mixtures of linear pUC19 and the 18-mer in 50 m*M* histidine containing: (a), 20 m*M* NaCl, $I=10.2$ μA; (b), 30 m*M* NaCl, $I=13.6$ μA; (c), 50 m*M* NaCl, $I=24.0$ μA. In all cases, $E=50$ V/cm.

conductivities of the anion and cation are approximately equal [16], minimizing any peak distortion caused by differing rates of migration of the counterions and co-ions to different electrodes. Typical results observed in solutions containing 50 m*M* KBr–50 m*M* histidine are illustrated in Fig. 6. The 18-mer (Fig. 6a) and linear pUC19 (Fig. 6b) eluted as two widely separated peaks in this buffer medium, even though single peaks were observed in 50 m*M* NaCl–50 m*M* histidine (compare Figs. 3c and 4c). The electropherogram of the DNA mixture in 50 m*M* KBr/50 m*M* histidine (Fig. 6c) was approximately the sum of the individual components, except that the peak corresponding to the 18-mer (elution time ~20 min) was broadened. Similar results were observed in solutions with other KBr concentrations (30–60 m*M* KBr–50 m*M* histidine).

Since the increased conductivity of the solution made it impossible to add more than 60 m*M* KBr to 50 m*M* histidine to try to obtain single peaks in the electropherograms, the histidine concentration was decreased to 25 m*M*, with the results illustrated in Fig. 7. In 50 m*M* KBr–25 m*M* histidine, the 18-mer migrated as a single peak (Fig. 7a). Two peaks were observed for linear pUC19 (Fig. 7b). A mixture of the two DNAs (Fig. 7c) exhibited peaks corresponding to each individual DNA as well as a small, slowly migrating peak eluting at ~36 min. The absolute mobilities observed in the various KBr–histidine solutions are compiled in Table 1.

3.5. Divalent salts

The DNA samples were also studied in solutions

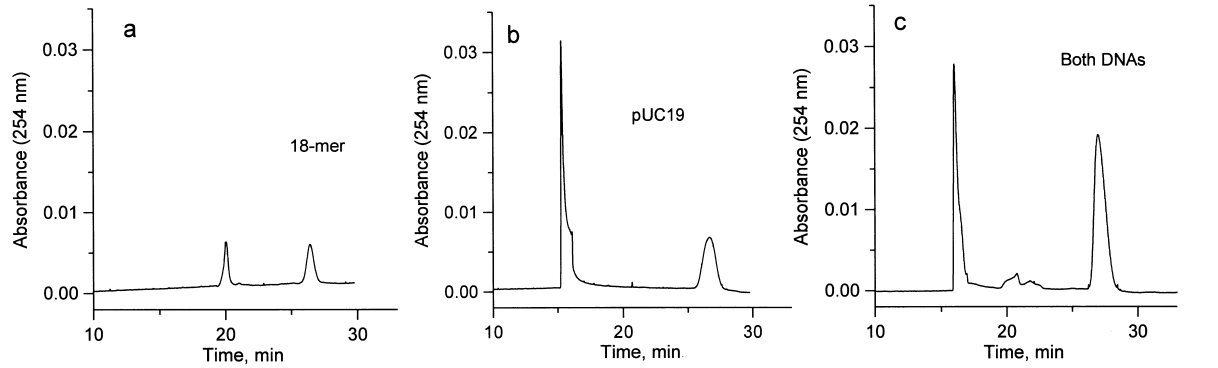

Fig. 6. Electropherograms observed in 50 m*M* KBr–50 m*M* histidine for (a), the 18-mer; (b), linear pUC19; (c), a mixture of the two DNAs. In all cases, $E=50$ V/cm, $I=28.5$ μA.

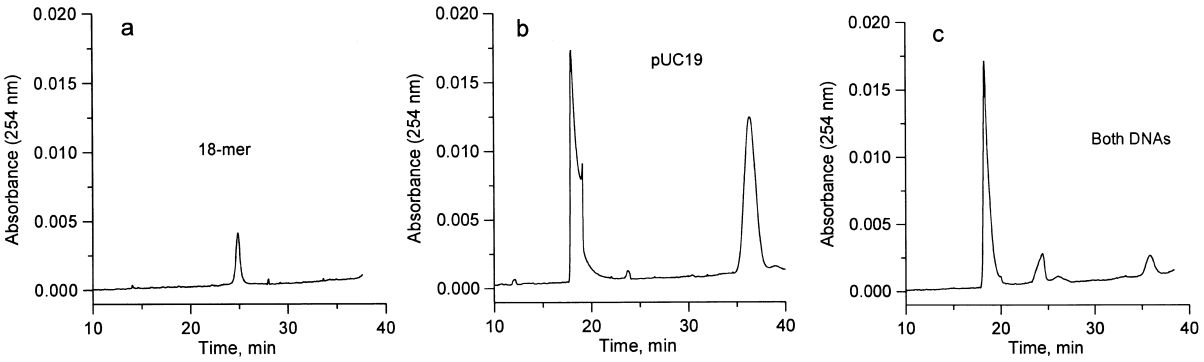

Fig. 7. Electropherograms observed in 50 m*M* KBr–25 m*M* histidine for (a), the 18-mer; (b), linear pUC19; (c), a mixture of the two DNAs. In all cases, $E=50$ V/cm, $I=28.1$ μA.

with divalent cations or anions added to the isoelectric histidine buffer. Because of the increased conductivity of these solutions, it was not possible to add more than 30 m*M* Na_2SO_4, $MgCl_2$, or $CaCl_2$ to the background histidine buffer. The results obtained in 30 m*M* Na_2SO_4–50 m*M* histidine (not shown) were similar to those observed with 50 m*M* KBr–50 m*M* histidine (Fig. 6). The results observed with 30 m*M* $MgCl_2$ or $CaCl_2$ were similar; typical electropherograms observed in 30 m*M* $CaCl_2$–50 m*M* histidine are illustrated in Fig. 8. Two peaks were observed for the 18-mer (Fig. 8a) and linear pUC19 (Fig. 8b). The electropherogram observed for the mixture was approximately the sum of the individual spectra, as shown in Fig. 8c. Typical mobilities obtained in 50 m*M* histidine buffer containing various divalent cations and anions are summarized in Table 1.

4. Discussion

4.1. DNA–histidine complexes

The electropherograms observed for the 18-mer, linear pUC19 and their mixture in isoelectric histidine buffers were highly anomalous. The monodisperse DNAs (and their mixture) eluted as two components – a broad, relatively rapidly migrating peak eluting at ~16 min and a slower, relatively sharp peak eluting at 26–33 min, depending on the particular DNA (Fig. 2). The contrast between these electropherograms and those exhibited by the same DNAs in TAE buffer (Fig. 1) or TBE buffer [7] suggests that DNA–histidine complexes are formed in isoelectric histidine buffers.

The formation of DNA–histidine complexes in isoelectric histidine is probably due to the extended

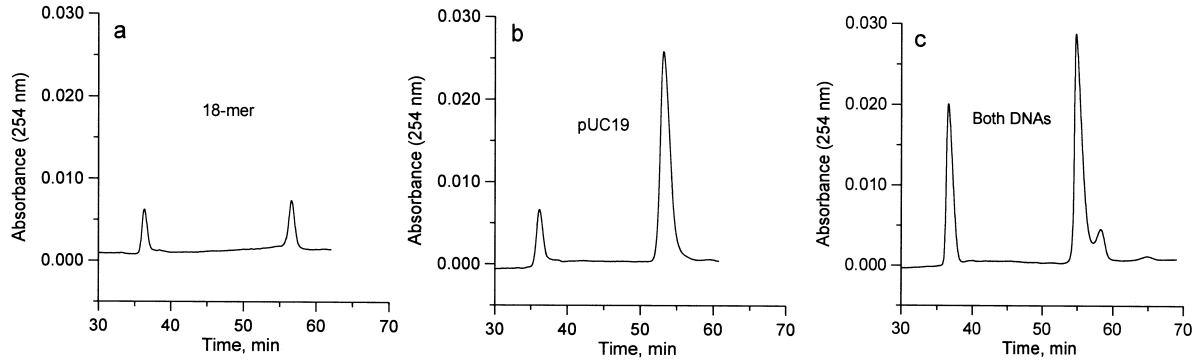

Fig. 8. Electropherograms observed in 30 m*M* $CaCl_2$–50 m*M* histidine for (a), the 18-mer; (b), linear pUC19; (c), a mixture of the two DNAs. In all cases, $E=50$ V/cm, $I=23.6$ μA.

double layer around the DNA molecules in solutions of very low ionic strength. The Debye screening parameter, κ^{-1}, which is a measure of the thickness of the ion atmosphere, is estimated to be 30 Å in 10 m*M* NaCl [17]; it is probably of similar magnitude in 10 m*M* NaCl–50 m*M* histidine and much larger in 50 m*M* histidine buffer without added salt. When the thickness of the ion atmosphere is so large, the electrostatic potential around the DNA molecules extends far into the solution. Large ions, such as histidine, which would normally be sterically excluded from the DNA grooves [18], would be able to interact electrostatically with the extended ion atmosphere. Once attracted into the double layer, the positively charged amino groups of histidine may have formed chelates with the negatively charged DNA phosphate groups [8], leading to complex formation. It seems likely that histidine residues bound to the phosphate groups by such charge–charge interactions would also interact with each other, possibly via $\pi-\pi$ stacking interactions, to form an extensive layer on the outside of the DNA helix. Similar outside-bound complexes are formed by planar aromatic dyes [19,20].

4.2. Effect of neutral salts on the formation/stability of DNA–histidine complexes

The binding of the histidine molecules to the DNA phosphates would be expected to decrease in the presence of added neutral salts, because the thickness of the ion atmosphere decreases with increasing ionic strength [17]. In addition, the more highly charged monovalent and divalent cations in the added salts would be preferentially attracted to the negatively charged phosphate groups, displacing the bound histidine residues. In accordance with these expectations, adding 50 m*M* NaCl to 50 m*M* isoelectric histidine buffer effectively eliminated DNA–histidine complex formation, and the 18-mer and linear pUC19 migrated as single, relatively symmetric peaks in this buffer medium (Figs. 3c and 4c). Hence, the DNA–histidine complexes appear to be stabilized by electrostatic interactions.

KBr was not as effective as NaCl in eliminating DNA–histidine complex formation, because two peaks were observed for both the 18-mer and linear pUC19 in solutions containing 30–60 m*M* KBr–50 m*M* histidine (Fig. 6). KBr may be less effective than NaCl in destabilizing the DNA–histidine complexes because the larger K^+ ions do not interact as strongly as Na^+ ions with the phosphate residues [21,22].

The stability of the DNA–histidine complexes also depended on DNA molecular mass. Linear pUC19 migrated as a single peak in isoelectric histidine buffer containing 20–50 m*M* NaCl (Fig. 3), suggesting that pUC19–histidine complexes did not form or were not stable in these solutions. However, the 18-mer exhibited two peaks in 30 m*M* NaCl–50 m*M* histidine, indicating the presence of DNA–histidine complexes in this buffer medium. The opposite behavior was observed in KBr–histidine solutions. The 18-mer migrated as a single peak in 50 m*M* KBr–25 m*M* histidine (Fig. 8a), indicating the absence of complexes, while linear pUC19 exhibited two peaks, indicating complex formation, under the same conditions (Fig. 8b). Thus, the stability of the DNA–histidine complexes appears to be mediated by DNA size as well as the concentration and type of low-molecular-mass electrolyte.

Divalent cations such as Mg^{2+} or Ca^{2+} were not able to destabilize the DNA–histidine complexes over the available range of divalent ion concentrations (10–30 m*M*), as illustrated in Fig. 8. The 18-mer and linear pUC19 exhibited two peaks in 30 m*M* $CaCl_2$–50 m*M* histidine; the mixture contained three peaks and was the sum of the two individual spectra. It is possible that the divalent cations acted as bridges between the histidine residues and/or the DNA molecules, stabilizing the DNA–histidine complexes. Alternatively, it is possible that the added concentration of divalent cations was too small to disrupt the DNA–histidine complexes. Further experiments are needed to answer this question.

4.3. Dependence of the electrophoretic mobilities on added salt and identification of the two peaks in the electropherograms

The apparent absolute electrophoretic mobilities observed for the 18-mer, linear pUC19 and mixtures of the two DNAs in 50 m*M* histidine buffer with and without added monovalent and divalent ions are summarized in Table 1. For the 18-mer, the absolute mobility was approximately the same in 50 m*M*

histidine and in 50 m*M* histidine plus 10 m*M* NaCl or 10 m*M* KBr. The equivalence of the mobilities is surprising, since electrophoretic mobilities are predicted theoretically to decrease with increasing solution conductivity [14,15,23], and the conductivity of 50 m*M* isoelectric histidine increased about threefold upon adding 10 m*M* NaCl or 10 m*M* KBr to the solution. Even more surprisingly, the mobility of linear pUC19 increased upon adding 10 m*M* NaCl or 10 m*M* KBr to 50 m*M* histidine buffer, just the opposite of the expected effect. The results suggest that the DNA in the broad fast peaks observed in isoelectric histidine buffer (without added salt) contained some histidine that was in rapid exchange with other histidine molecules in the solvent. Under such conditions, a peak with a mobility intermediate between that of the isolated molecule and its complex would be observed, because the average mobility is weighted by the fraction of time that the DNA migrates as a free (uncomplexed) molecule [24].

Two relatively sharp peaks were usually observed in the electropherograms measured with neutral salts added to isoelectric histidine buffer (Figs. 4–8). The mobility of the faster-migrating peak in each of the electropherograms decreased approximately as the logarithm of the conductivity of the solvent, as illustrated in Fig. 9 for NaCl–histidine solutions. Such a decrease is predicted theoretically [15] and has been observed experimentally for DNA [6,7,21,22]. The rate of decrease of the mobility with increasing salt concentration was approximately independent of DNA molecular mass (Fig. 9), again in agreement with theoretical predictions [15]. Hence, it seems likely that the faster migrating peaks in the various electropherograms can be assigned to the elution of the DNA molecules.

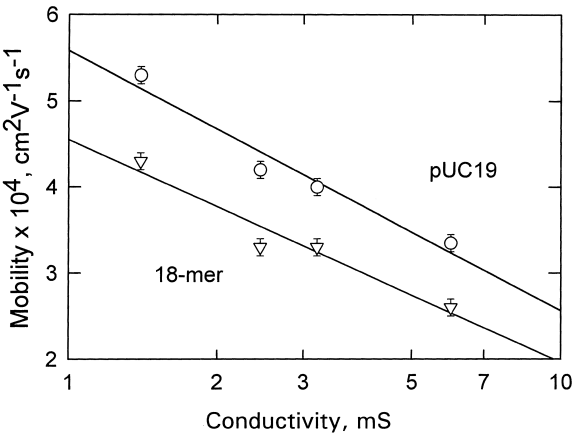

Fig. 9. Dependence of the electrophoretic mobility on the logarithm of the conductivity of the solvent linear pUC19 (○) and the 18-mer (▽). All solutions contained 50 m*M* histidine plus varying quantities of NaCl; $E=50$ V/cm. The solid lines were calculated by linear regression.

The mobility of the more slowly migrating peak in each electropherogram (when present) was approximately independent of the concentration of added salt, as shown in Table 1. Since the slow peaks were not observed when high concentrations of neutral salt were added to isoelectric histidine buffer (see, e.g., Figs. 3, 4a and c and 7a), and were never observed when sample buffer alone (without DNA) was injected into the capillary, it seems likely that they can be attributed to the migration of DNA–histidine complexes. The fact that the mobilities of the slow peaks were independent of solution conductivity suggests that the composition of the DNA–histidine complexes varied in solutions with different salt concentrations.

The following approximate calculation illustrates this point. The electrophoretic mobility of a polyelectrolyte is predicted theoretically to vary as:

$$\mu = q/f \tag{2}$$

where q is the effective charge and f is the translational friction coefficient [15,23,25,26]. The net charge of the DNA–histidine complexes should be approximately equal to that of the DNA alone, since histidine is electrically neutral at its isoelectric pH. Therefore, the decrease in mobility of the complexes should be due primarily to a change in the frictional coefficient, f. For rigid, rod-like molecules like the 18-mer studied here, $f \sim M^{0.8}$, where M is the DNA molecular mass. Larger DNA molecules such as linear pUC19 are worm-like coils, which are free draining in electrophoresis [7,15,25,26]. Under such conditions, $f \sim M^{1.0}$. Hence, the ratio of the mobilities of the fast (DNA) and slow (complex) peaks in the electropherograms can be used to estimate the molecular mass of the complexes, using the relation:

$$\frac{\mu_{\mathrm{DNA}}}{\mu_{\mathrm{complex}}} = \left(\frac{M_{\mathrm{complex}}}{M_{\mathrm{DNA}}}\right)^{x} \tag{3}$$

where x is 0.8 (for the 18-mer) or 1.0 (for pUC19). Eq. 3 also contains the implicit assumption that the frictional coefficients of the DNAs and their histidine complexes exhibit the same dependence on x. The apparent molecular mass of the complex, $M_{complex}$, can then be used to estimate the number of moles of histidine in the complex, from which the number of moles of histidine per nucleotide residue ([His]/[DNA-P]) can be estimated. The results of such a calculation are given in Table 2 for a series of KBr–histidine solutions. The results suggest that there is a progressive decrease in the mole ratio of bound histidine residues as the KBr concentration is increased. Such a decrease could obscure the expected decrease of the electrophoretic mobility with increasing solution conductivity.

The estimated [His]/[DNA-P] ratios in Table 2 suggest that histidine forms an extensive layer around the outside of the DNA helix, much as planar aromatic dyes form extensive outside-bound arrays on the DNA helix [19,20]. However, the actual numerical values in Table 2 cannot be taken too literally, because they depend on the assumption that counterion condensation is unaffected by histidine complexation. This is a reasonable approximation, since counterion condensation is virtually independent of ionic strength over a wide range of ionic strengths [26]. However, if histidine complexation were to induce an increase in counterion condensation, decreasing the effective net charge of the DNA molecules, the DNA–histidine complexes would migrate more slowly than the parent DNA molecules because of the reduced net charge. In such a case, the [His]/[DNA-P] ratios in the various complexes would be lower than estimated in Table 2.

Table 2
Approximate composition of DNA–histidine complexes in 50 m*M* isoelectric histidine buffers containing added KBr

KBr (m*M*)	[His]/[DNA-P][a]	
	18-mer	Linear pUC19
10	1.9	2.6
30	1.5	2.0
50	0.9	1.5
60	–	1.9

[a] Molar ratio of histidine residues to DNA nucleotide bases, assuming that the decrease in mobility of the complexes is due entirely to an increase in mass.

The [His]/[DNA-P] ratio might also be lower than indicated in Table 2 if the histidine residues and/or added cations could act as bridges between the DNA molecules, in effect increasing the average molecular mass of the DNA. In such a case, large dipolar arrays of DNA–histidine complexes might have formed because of electrohydrodynamic instabilities in the capillary, similar to the dipolar arrays observed for very high-molecular-mass DNAs in TBE buffer [27]. Such dipolar arrays migrate in widely separated clusters in the capillary, even though the DNA itself is monodisperse. The DNA molecules used in this study were much too small to form dipolar arrays, but the DNA–histidine aggregates might have been large enough to form such structures.

The electrophoretic mobilities observed for the 18-mer and linear pUC19 in 30 m*M* $CaCl_2$–50 m*M* histidine were ~two-fold lower than the mobilities observed in solutions containing 30 m*M* NaCl, KBr or Na_2SO_4, as shown in Table 1. Such a decrease is expected from counterion condensation theory, which posits that the effective charge on the DNA phosphates is proportional to $1/Z$, where Z is the counterion valence [26]. Hence, from Eq. 2, the electrophoretic mobility is predicted to decrease by approximately a factor of 2, as observed, when divalent counterions are added to the background electrolyte. Similar decreases in mobility have been observed in free solution [7] and in gels [28] upon adding divalent cations to the running buffer.

5. Conclusions

The studies described here suggest that DNA molecules form complexes with histidine molecules in isoelectric histidine buffers, giving rise to peak distortion and splitting in the electropherograms. The faster-migrating peak in each electropherogram can be attributed to the migration of the DNA molecules, because the mobilities of the fast peaks decreased with increasing solution conductivity, as expected theoretically [15].

The slower-migrating peak in each electropherogram can probably be attributed to the migration of DNA–histidine complexes. The mobilities of these peaks were approximately independent of solution conductivity, most likely because the composition of

the DNA–histidine complexes varied in solutions with different concentrations of neutral salts, obscuring any dependence of the mobility on solution conductivity.

The DNA–histidine complexes could be disrupted by adding a sufficient concentration of monovalent cations to isoelectric histidine buffer, giving rise to electropherograms containing a single DNA peak. Hence, the complexes appear to be stabilized by electrostatic interactions. The stability of the DNA–histidine complexes also depends on the molecular mass of the DNA and on the concentration and type of added neutral salt. Na^+ ions were more effective than K^+ ions in destabilizing the DNA–histidine complexes; divalent cations were not able to disrupt the complexes over the available range of divalent ion concentrations.

Acknowledgements

The expert assistance of Kurt Strutz and Andrea Fastenow in sample preparation is gratefully acknowledged. Financial support for N.C.S. from the National Institute of General Medical Sciences (Grant 29690) is also acknowledged. P.G.R. is supported by grants from AIRC (Associazione Italiana Ricerca sul Cancro), by the European Union (Bio Med 2, grant No. BMH4-CT97-2627), by Telethon-Italy (grant No. E.555) and from POP Calabria 94-98.

References

[1] S. Hjerten, L. Valtcheva, K. Elenbring, J.-L. Liao, Electrophoresis 16 (1995) 584–594.
[2] C. Gelfi, M. Perego, P.G. Righetti, Electrophoresis 17 (1996) 1470–1475.
[3] A.V. Stoyanov, C. Gelfi, P.G. Righetti, Electrophoresis 18 (1997) 717–723.
[4] M. Perego, C. Gelfi, A.V. Stoyanov, P.G. Righetti, Electrophoresis 18 (1997) 2915–2920.
[5] P.G. Righetti, C. Gelfi, M. Perego, A.V. Stoyanov, A. Bossi, Electrophoresis 18 (1997) 2145–2153.
[6] B.M. Olivera, P. Baine, N. Davidson, Biopolymers 2 (1964) 245–257.
[7] N.C. Stellwagen, C. Gelfi, P.G. Righetti, Biopolymers 42 (1997) 687–703.
[8] C. Gelfi, D. Mauri, M. Perduca, N.C. Stellwagen, P.G. Righetti, Electrophoresis 19 (1998) 1704–1710.
[9] A.R. Volkel, J. Noolandi, Macromolecules 28 (1995) 8182–8189.
[10] U. Mohanty, N.C. Stellwagen, Biopolymers, in press.
[11] N.C. Stellwagen, Biochemistry 22 (1983) 6180–6185.
[12] D.L. Holmes, N.C. Stellwagen, Electrophoresis 11 (1990) 5–15.
[13] G.D. Fasman (Ed.), Handbook of Biochemistry and Molecular Biology, Proteins Vol. I, CRC Press, Cleveland, OH, 1976, 196.
[14] S. Hjerten, Electrophoresis 16 (1995) 584–594.
[15] G.S. Manning, J. Phys. Chem. 85 (1981) 1506–1515.
[16] R.A. Robinson, R.H. Stokes, Electrolyte Solutions, Butterworths, London, 1959, p. 463.
[17] C. Tanford, Physical Chemistry of Macromolecules, Wiley, New York, 1961, p. 500.
[18] G. Lamm, L. Wong, G.R. Pack, Biopolymers 35 (1994) 227–237.
[19] D.F. Bradley, M.K. Wolf, Proc. Natl. Acad. Sci. USA 45 (1959) 944–952.
[20] H.J. Li, D.M. Crothers, J. Mol. Biol. 39 (1969) 461–477.
[21] P.D. Ross, R.L. Scruggs, Biopolymers 2 (1964) 79–89.
[22] P.D. Ross, R.L. Scruggs, Biopolymers 2 (1964) 231–236.
[23] J.T.G. Overbeek, P.H. Wiersema, in: M. Bier (Ed.), Electrophoresis, Academic Press, New York, 1967, pp. 1–52.
[24] K. Shimura, D. Kasai, Anal. Biochem. 251 (1997) 1–16.
[25] P.D. Grossman, in: P.D. Grossman, J.C. Colburn (Eds.), Capillary Electrophoresis, Academic Press, San Diego, CA, 1992, pp. 111–132.
[26] G.S. Manning, Q. Rev. Biophys. 11 (1978) 179–246.
[27] L. Mitnik, C. Heller, J. Prost, J.L. Viovy, Science 167 (1995) 219–222.
[28] C. Ma, V.A. Bloomfield, Biopolymers 35 (1995) 211–216.